

## UTILIZING BIOMIMETIC OLIGOPEPTIDES TO PROBE FIBRONECTIN-INTEGRIN BINDING AND SIGNALING IN REGULATING MACROPHAGE FUNCTION *IN VITRO* AND *IN VIVO*

Weyuan John Kao<sup>1,2</sup> and Yiping Liu<sup>1</sup>

<sup>1</sup> Division of Pharmaceutical Sciences of the School of Pharmacy, <sup>2</sup> Department of Biomedical Engineering of the College of Engineering, University of Wisconsin – Madison, Madison, WI, USA

### TABLE OF CONTENTS

1. Abstract
2. Introduction
3. Materials and Methods
  - 3.1. Synthesis of polymer substrates containing biomimetic oligopeptides
  - 3.2. *In vitro* macrophage and FBGC assays
  - 3.3. *In vivo* cage implantation study
  - 3.4. Statistical analysis
4. Results and Discussions
  - 4.1. *In vitro* macrophage adhesion and FBGC formation
  - 4.2. *In vivo* macrophage adhesion and FBGC formation
  - 4.3. Probing the intracellular signaling with biomimetic oligopeptides
5. Acknowledgements
6. References

### 1. ABSTRACT

Biomimetic oligopeptides were employed to elucidate the molecular mechanisms of fibronectin-integrin interaction in regulating macrophage function. Oligopeptides were designed based on the functional structure of fibronectin and grafted onto a polymer network containing polyethyleneglycols. Macrophage adhesion was independent of the peptide identity that contained sequence RGD, PHSRN, PRRARV, or combinations thereof in an integrin-dependent fashion *in vitro*. However, integrin-dependent foreign body giant cell (FBGC) formation *in vitro* was highly dependent on both RGD and PHSRN in a single peptide formulation and with a specific orientation. *In vivo* results showed that peptide identity played a minimal role in modulating the host inflammatory response and adherent macrophage density. RGD-containing peptides mediated a rapid FBGC formation by 4 days of implantation by significantly increasing both the number of macrophages that participate in the cell fusion process and the rate of cell fusion. Both RGD and PHSRN domains were important in mediating FBGC formation at later implantation periods. *In vitro* intracellular signaling studies revealed that the requirement of protein tyrosine kinase and serine/threonine kinase activation and cross-talk compensation for macrophage adhesion dynamically varied with surfaces and culture time. Protein kinase C-dependent adhesion was related to RGD and PHSRN sequences, and to the sequence orientation thereof in a form of GGGRGDGGGGGPHSRNG. Furthermore, we observed a multiple effect of the mitogen-activated protein kinase/extracellular-signal-regulated kinase signaling factor in mediating macrophage adhesion, which depended on the

method of ligand immobilization. These findings represent a mechanistic correlation between the role of substrates and protein functional architectures in ligand-receptor recognition and post-ligation signaling events that control cellular behavior *in vitro* and *in vivo*.

### 2. INTRODUCTION

The host inflammatory reaction is a normal response to injury and the presence of foreign objects. The magnitude and duration of the inflammatory process have a direct impact on biomaterial biostability and biocompatibility, hence affecting the efficacy of biomedical devices (1,2). Central in directing host inflammatory and immune processes and healing are mononuclear phagocytic and reticuloendothelial systems (such as blood monocytes and polymorphonuclear leukocytes (PMN), tissue macrophages and macrophage-derived multinucleated foreign body giant cells (FBGC), connective tissue histiocytes and osteoclasts). Therefore, the response of these cells of macrophage lineage to biomaterials is important in understanding material-mediated host reaction and improving device performance. Several characteristic phagocyte functions are identified as critical events in the material-host interaction. First, phagocytes recognize adsorbed proteins on the biomaterial surface and may adhere via several adhesion ligand-receptor superfamilies. Cell adhesion mediated by ligand-receptor complexation may be modulated by the presence of cytokines, growth factors, and other biologically active molecules (3-8). Second, the process of blood-derived macrophage

activation and fusion to form FBGCs is unique to the macrophage phenotype. FBGCs are utilized as a histopathology marker for chronic inflammation and host foreign body reaction (2). FBGCs have been demonstrated on biomaterials *in vivo*. The rate of material degradation underneath giant cells increased markedly (9). However, the molecular mechanisms involved in FBGC formation remain unclear. Third, activated macrophages release cytokines, growth factors, and other bioactive agents to modulate the function of other cell types such as fibroblasts and endothelial cells in the host environment (3,6,7,10).

The functional architecture of plasma and extracellular matrix protein fibronectin offers a working model to probe the interaction between proteins and extracellular membrane receptors in modulating macrophage behavior. Fibronectin has been found to adsorb on clinically-relevant biomaterials and play an important role in the host foreign body reaction (3,5). Several signaling transduction events initiated by fibronectin-integrin complexation are directly involved in modulating macrophage behavior (11-16). Although FBGCs express  $\alpha$ -2,  $\alpha$ -4,  $\beta$ -1, and  $\beta$ -3 integrin subunits (17,18), the involvement of fibronectin and integrins in FBGC formation remains unknown. Furthermore, there is no direct correlation between the cell-binding structure of fibronectin and the macrophage function mediated by fibronectin-integrin interaction. Hence, we are interested in the role of various bioactive regions of fibronectin in ligand-receptor recognition and subsequent macrophage development. RGD and PHSRN amino acid sequences, which are located in the FIII-10 and FIII-9 modules, respectively, of the central cell-binding domain and the PRRARV sequence of the C-terminal heparin-binding domain of fibronectin (19,20) are chosen for exploration in the current study. RGD (21) and PHSRN (22) are present on adjacent loops of two connecting FIII modules and bind synergistically to various integrins containing a myriad of  $\alpha$ - and  $\beta$ -subunits (i.e., RGD binds to  $\alpha$ -(2,3,4,5,7,8,v)/ $\beta$ -1,  $\alpha$ -v/ $\beta$ -(1,3,5,6,8),  $\alpha$ -IIb/ $\beta$ -3; whereas PHSRN binds to  $\alpha$ -5/ $\beta$ -1,  $\alpha$ -(IIb,v)/ $\beta$ -3) (23-26). The heparin-binding domain of fibronectin that contains the PRRARV sequence also binds directly with integrins; however, the precise interaction involved in this association remains unclear (20,26,27).

## 3. MATERIALS AND METHODS

### 3.1. Synthesis of polymer substrates containing biomimetic oligopeptides

Fibronectin-derived peptides were designed from RGD, PHSRN, and PRRARV sequences. We estimated the distance between RGD and PHSRN sequences from the structural coordinates of native fibronectin archived in the SwissProt Database<sup>®</sup> (28). A poly-glycine hexamer ( $G_6$ ) of approximately the same length was used to link each domain at all possible orientations. A tri-glycine ( $G_3$ ) sequence was used as a spacer at the N-terminus for each peptide to promote peptide chain flexibility since ligand mobility and accessibility impact ligand-receptor association. Fibronectin-derived peptides synthesized

were:  $G_3$ RGDG,  $G_3$ PHSRNG,  $G_3$ RGDG $_6$ PHSRNG,  $G_3$ PHSRNG $_6$ RGDG,  $G_3$ RGDG $_6$ PRRARV,  $G_3$ PRRARV $_6$ RGDG, and  $G_3$ RDGG which was used as a control. All oligopeptides were synthesized by the University of Wisconsin Biotechnology Center Peptide Synthesis Facility (Madison, WI). Peptide purity was 87-99% as determined by HPLC and mass spectroscopy. Oligopeptides were covalently grafted at the N-terminus onto polyethyleneglycol-based polymer networks. The synthesis and characterization of the monomethoxypolyethyleneglycol monoacrylate (mPEGMA), acrylic acid (Ac), and trimethylolpropane triacrylate (TMPTA) copolymer network have been previously described in detail (28,29). The network mediated a low level of adhesion by human fibroblasts, endothelial cells, macrophages and murine macrophages for a long duration of culture in the presence of serum proteins. Detailed procedure and characterization of protein and peptide grafting have been previously described (28,29). The grafted peptide surface density was found to be dependent on the number of amino acids per peptide. For example, pentapeptides were grafted at  $66 \pm 5$  pmol/cm<sup>2</sup> surface density, whereas peptides containing 20 residues were grafted at approximately one third of that surface density. Hence we hypothesized that the density of grafted peptides is lower than that of pre-adsorbed TCPS. Furthermore, serum coated TCPS will likely to have more ligands available for cell-membrane receptor binding than the density of ligands covalently grafted onto the network.

### 3.2. *In vitro* macrophage and FBGC assays

Monocytes were isolated from the blood of medication-refrained healthy adults via a density-gradient non-adhesion method (30). Each test sample was placed in a well of a 24-well tissue culture polystyrene (TCPS) plate and incubated with  $10^6$  cells suspended in 1 ml of RPMI culture medium containing 10% autologous serum. Prior to the culture incubation, cells were pre-treated with one of the following inhibitors: protein tyrosine kinase (PTK) inhibitor (AG82 at 300 micro-M, which was chosen because when 150, 300, or 1000 micro-M concentrations were employed, 300 micro-M was found to be the optimal dose regarding to the inhibition effect and without inducing cell death for up to 120 h of incubation as determined by trypan blue exclusion test), protein serine/threonine kinase (PSK) inhibitor (H-7 at 100 micro-M to extensively inhibit protein kinases-C, -A, and -G per supplier's instruction), Src-family kinase inhibitor (Lavendustin A at 2 micro-M), protein kinase C (PKC) inhibitor (Myristoylated EGF-R Fragment at 10 micro-M, IC<sub>50</sub> = 5 micro-M that inhibits the catalytic fragment by binding to PKC-free but not to the complex PKC-ATP at the protein-substratum binding site), phosphoinositide-3 kinase (IP3-K) inhibitor (Wortmannin at 100 nano-M that blocks the catalytic activity of PI3 kinase without affecting the upstream signaling events), or "mitogen-activated protein (MAP) kinase/extracellular-signal-regulated kinase" (MEK) inhibitor (PD98059 at 100 micro-M that selectively blocks the activity of MAP kinases MAPKK, ERK kinase, or MEK by inhibiting the activation of MAP kinase and the subsequent phosphorylation of MAP kinase substrates,) for 1 h in suspension under a constant gentle agitation. Also prior to the culture incubation, cells were pre-treated with monoclonal anti-human integrin  $\beta$ -3

**Table 1.** Adherent macrophage density on mPEGMA-co-Ac-co-TMPTA networks grafted with fibronectin-derived peptides (cells pretreated with anti-integrin antibody)

Peptide	No antibody treatment		Anti-integrin beta-3 treatment		Anti-integrin beta-1 treatment	
	Culture time (hr)					
	24	168	24	168	24	168
G <sub>3</sub> RGDG	38±6	16±8	5±1*	4±2*	0±0*	0±0*
G <sub>3</sub> PHSRNG	24±3	12±7	7±3*	4±2	0±0*	0±0*
G <sub>3</sub> PRRARVG	30±5	12±5	7±4*	4±2*	1±1*	1±0*
G <sub>3</sub> RGDG <sub>6</sub> PHSRNG	27±3	9±3	7±3*	4±3	0±0*	0±0*
G <sub>3</sub> PHSRNG <sub>6</sub> RGDG	31±4	10±3	8±4*	4±1*	0±0*	0±0*
G <sub>3</sub> RGDG <sub>6</sub> PRRARVG	31±4	9±3	6±1*	5±1	0±0*	0±0*
G <sub>3</sub> PRRARVG <sub>6</sub> RGDG	15±2	6±2	5±2*	3±2	0±0*	0±0*
TCPS	40±5	13±2	27±10	19±4	6±2*	7±2*

All values expressed in ( $\times 100$  macrophage/mm<sup>2</sup>), mean  $\pm$  s.e.m., n = 3 to 5. \* represents  $p < 0.05$  vs respective values of “no antibody treatment” controls.

neutralizing antibody (25E11, purified IgG2a isotype at 60 micro-gram/ml) (28) or monoclonal anti-human integrin beta-1 neutralizing antibody (JB1 purified IgG isotype at 60 micro-gram/ml) (28) for 1 h in suspension under a constant gentle agitation. Vehicle, isotype IgG or IgG2a, and no treatment were utilized as controls. Treated cells were then cultured in serum-containing media with the addition of aforementioned inhibitor or vehicle control. The culture medium was exchanged with fresh medium with the same component every 96 h.

An established *in vitro* FBGC assay (30) was employed to determine the effect of fibronectin and grafted peptides on FBGC formation. Under the culture condition described, FBGCs containing up to 50 nuclei/cell formed consistently on TCPS. Briefly, 10<sup>6</sup> freshly isolated monocytes were pretreated with or without anti-integrin antibody or controls as stated above then incubated with samples in 1 ml of RPMI containing 20% autologous serum. At 96 and 168 hr, the medium was changed to RPMI with 20% heat-inactivated (30 min at 57 °C) autologous serum + 10 nano-gram/ml of recombinant human interleukin-4 + 5 nano-gram/ml of recombinant human granulocyte-macrophage colony stimulating factor (Genzyme) + anti-integrin antibody as stated above. Each adherent cell with three or more nuclei per cell was defined as a FBGC. At 240 hr, adherent macrophage and FBGC density and size were quantified based on measurements from five randomly selected fields using a computerized video analysis system coupled to a phase contrast optical microscope.

### 3.3. *In vivo* cage implantation study

The well-established subcutaneous cage-implant system was utilized to study the effect of implanted materials on the host foreign body reaction (31-33). Briefly, polymer samples were inserted under sterile conditions into an autoclaved cylindrical cage measured 3.5-cm long, 1 cm in diameter, and constructed from medical grade stainless steel wire mesh. Cages containing various polymer samples were subcutaneously implanted at the back of 3-month old female Sprague-Dawley rats. Empty cages were implanted as controls. The inflammatory exudate that collects in the cage was withdrawn at 4, 7, 10, 14, and 21 days post-implantation and analyzed for the quantitative evaluation of cellular and humoral responses to

the test material using standard hematology techniques (33). Specifically, the distribution of lymphocyte, monocyte, and PMN subpopulations in the exudate was determined. The presence of a high concentration of PMNs in the inflammatory exudate indicates an acute inflammatory response, which occurs from the onset of implantation and attenuates with time. This is followed by the chronic inflammatory response, which is characterized by the presence of a high concentration of monocytes and lymphocytes in the exudate. No PMN ( $0 \pm 0$  cells/ml) was observed for all materials and controls at all retrieval times. At 4, 7, 14, 21, 35, and 70 days post-implantation, test polymer samples were retrieved and adherent cell morphology and density were quantified using a video analysis system coupled to a light microscope.

### 3.4. Statistical analysis

All experimental data are expressed in mean  $\pm$  standard error of the mean (s.e.m.). Statistical analyses were performed with SigmaStat 2.03 (SPSS Science). Comparative analyses (n = 3) were determined using Student's *t*-test at 95% confidence level. Differences were considered to be statistically significant at  $p$  value  $< 0.05$ .

## 4. RESULTS AND DISCUSSIONS

### 4.1. *In vitro* macrophage adhesion and FBGC formation

We found previously that serum fibronectin modulated macrophage adhesion and the extent (i.e., size) of FBGC formation on TCPS in the presence of serum proteins (28). In the current study, macrophages adhered to all peptide-grafted mPEGMA-co-Ac-co-TMPTA networks with relatively subtle differences between adhesion mediated by peptides containing sequence RGD, PHSRN, PRRARV, or combinations thereof (table 1). Beta-1 integrin subunit was essential in macrophage adhesion to peptide-grafted networks; whereas, beta-3 integrin subunit was less important (table 1). Macrophage adhesion to surfaces grafted with PRRARV-containing peptides was mediated primarily by the direct interaction with integrins. Networks grafted with peptides that contain RGD or PHSRN alone did not provide an adequate substrate for macrophage fusion to form FBGCs (table 2). However, the PHSRN synergistic site and the RGD site in a single oligopeptide provided a substrate for FBGC formation that was statistically comparable to that on the TCPS positive

**Table 2.** Macrophage-derived FBGC adherent density on mPEGMA-co-Ac-co-TMPTA networks grafted with fibronectin-derived peptides at 240 hr of FBGC culture (cells treated with anti-integrin antibody)

Peptides	No antibody treatment	Anti-integrin beta-3 treatment	Anti-integrin beta-1 treatment
G <sub>3</sub> RGDG	18 ± 9	0 ± 0	0 ± 0
G <sub>3</sub> PHSRNG	14 ± 9	0 ± 0	0 ± 0
G <sub>3</sub> PRRARVG	15 ± 9	0 ± 0	0 ± 0
G <sub>3</sub> RGDG <sub>6</sub> PHSRNG	16 ± 7	0 ± 0	0 ± 0
G <sub>3</sub> PHSRNG <sub>6</sub> RGDG	88 ± 38	30 ± 30	0 ± 0
G <sub>3</sub> RGDG <sub>6</sub> PRRARVG	14 ± 7	0 ± 0	0 ± 0
G <sub>3</sub> PRRARVG <sub>6</sub> RGDG	17 ± 9	0 ± 0	0 ± 0
TCPS	60 ± 20	90 ± 30	0 ± 0

All values expressed in FBGC/mm<sup>2</sup>, mean ± s.e.m., n = 3 to 6. For “no antibody treatment” group, all values were significantly lower ( $p < 0.05$ ) than that of TCPS and networks grafted with G<sub>6</sub>PHSRNG<sub>6</sub>RGDG.

control. This response was highly dependent upon the relative orientation between RGD and PHSRN. Surfaces grafted with peptides that contain PRRARV alone or in tandem with RGD in a single peptide formulation did not support FBGC formation. Furthermore, results showed that no-antibody and anti-beta-3 neutralizing antibody treated groups had a comparable FBGC density on TCPS. On most of the peptide-grafted network, no FBGC formation was observed in the anti-beta-3 antibody treated group. One notable exception was the peptide that contains the PHSRN and the RGD domain in the optimal orientation, namely G<sub>3</sub>PHSRNG<sub>6</sub>RGDG, on which anti-integrin beta-3 reduced FBGC formation by about 70%. When anti-beta-1 neutralizing antibody was utilized, no FBGC formation was observed on all samples.

Macrophages express an wide array of integrin dimers that bind with RGD or RGD/PHSRN sequences. FBGCs are important but poorly characterized cell type. Investigations to date have shown that FBGCs express alpha-2, alpha-4, beta-1, and beta-3 integrin subunits but indicate none of the possible dimers (i.e., alpha-2/beta-1, alpha-2/beta-3, alpha-4/beta-1, or alpha-4/beta-3) that can be expressed could interact with the PHSRN sequence. Hence, our results suggest the possible existence of RGD/PHSRN- and PHSRN-binding integrin-like receptors on FBGCs. It is also known that the first 160 amino acids of integrin beta-1, specifically the alpha-helix formed by residues 141 to 160, are critical in integrin-ligand recognition. The above findings suggest that the association between this region of the integrin beta-1 receptor and G<sub>3</sub>PHSRNG<sub>6</sub>RGDG, but not G<sub>3</sub>RGDG<sub>6</sub>PHSRNG, results in the necessary binding characteristic that determines the subsequent cellular event leading to FBGC formation. Activated integrin beta-1 or beta-3 intracellular domains stimulate cell migration, modulate proliferation and gene expression, induce the assembly of F-actin cytoskeleton, and localize the activity of focal adhesion kinase

pp125<sup>FAK</sup>. These cellular events may contribute to the process of FBGC formation.

#### 4.2. *In vivo* macrophage adhesion and FBGC formation

To extend our *in vitro* finding, we probed the role of RGD and PHSRN in modulating the host inflammatory response and macrophage behavior *in vivo*. Our results showed that peptide identity played a minimal role in modulating the host inflammatory response (Table 3) and adherent macrophage density (table 4). FBGC densities (table 5) for all test samples were comparable and were higher than respective values of G<sub>3</sub>RDGG or “no grafted peptide” controls at each retrieval time from 14 to 70 days post-implantation. The percentage of FBGC coverage (total FBGC area per total sample area) for surfaces grafted with G<sub>3</sub>RGDG, G<sub>3</sub>PHSRNG, G<sub>3</sub>RGDG<sub>6</sub>PHSRNG, G<sub>3</sub>PHSRNG<sub>6</sub>RGDG, G<sub>3</sub>RDGG nonspecific controls, and “no grafted peptide” negative controls was (38 ± 10, 61 ± 17), (59 ± 2, 79 ± 6), (69 ± 1, 93 ± 5), (46 ± 14, 65 ± 7), (18 ± 8, 28 ± 18), and (13 ± 8, 22 ± 12) for (35 days, and 70 days post-implantation) respectively. These results showed that networks grafted with fibronectin-derived peptides mediated an extensive FBGC coverage that increased with increasing implantation time. Specifically, surfaces grafted with G<sub>3</sub>RGDG<sub>6</sub>PHSRNG showed the highest FBGC coverage at about 90 percent of the total sample area when compared with other sample types and controls by 70 days of implantation. These *in vivo* findings indicate that the RGD motif, specifically in the configuration of G<sub>3</sub>RGDG or G<sub>3</sub>PHSRNG<sub>6</sub>RGDG but not G<sub>3</sub>RGDG<sub>6</sub>PHSRNG, modulates a rapid macrophage fusion to form FBGCs that is observed at the early stage of implantation (i.e., within 4 days of implantation). Both RGD and PHSRN motifs were important in mediating FBGC formation at the later implantation time (i.e., from 14 to 70 days of implantation). Furthermore, the PHSRN motif, specifically in the configuration of G<sub>3</sub>RGDG<sub>6</sub>PHSRNG but neither in G<sub>3</sub>PHSRNG nor G<sub>3</sub>PHSRNG<sub>6</sub>RGDG, was more important in modulating the extent of FBGC formation (i.e., percent coverage) at the later implantation time.

A previously developed mathematical model describing the *in vivo* kinetics of macrophage fusion to form FBGCs on biomaterials was employed to provide insights into the effect of peptide identity on FBGC formation (31). Specifically, two kinetic parameters were calculated based on results of the FBGC size-distribution at day 4, 7, 14, and 21 of implantation: (a) the density of adherent macrophages that participate in the FBGC formation and (b) the rate constant of cell fusion. Calculations showed that the density of adherent macrophages that participate in the FBGC formation was 127 ± 10, 100 ± 5, 62 ± 10, 123 ± 30, 53 ± 12, and 46 ± 10 macrophages/mm<sup>2</sup> for networks grafted with G<sub>3</sub>RGDG, G<sub>3</sub>PHSRNG, G<sub>3</sub>RGDG<sub>6</sub>PHSRNG, G<sub>3</sub>PHSRNG<sub>6</sub>RGDG, G<sub>3</sub>RDGG, or no grafted peptide, respectively. The rate constant of cell fusion ranged from 2.4 × 10<sup>-3</sup> to 5.6 × 10<sup>-3</sup> mm<sup>2</sup>cell<sup>-1</sup>week<sup>-1</sup> with a medium value of 4.0 × 10<sup>-3</sup>. The rate constant of cell fusion indicates that the cell fusion rate on surfaces grafted with G<sub>3</sub>PHSRNG, G<sub>3</sub>RGDG<sub>6</sub>PHSRNG,

**Table 3.** Total and differential leukocyte concentration in the inflammatory exudate of mPEGmA-co-Ac-co-TMPTA networks grafted with various fibronectin-derived oligopeptides

Peptide	Implantation (days)	Cell Concentration ( $\times 10^3$ cells/micro-l)		
		Total	Lymphocyte	Monocyte
G <sub>3</sub> RGDG	4	127 $\pm$ 25	71 $\pm$ 22	56 $\pm$ 5 §
	7	67 $\pm$ 13	24 $\pm$ 4 †	43 $\pm$ 9 §
	14	74 $\pm$ 18	21 $\pm$ 4	53 $\pm$ 25
	21	31 $\pm$ 8 †‡§	27 $\pm$ 8 †§	5 $\pm$ 1 †
G <sub>3</sub> PHSRNG	4	63 $\pm$ 32	25 $\pm$ 22 §	38 $\pm$ 17 §
	7	61 $\pm$ 9	25 $\pm$ 6	36 $\pm$ 3 §
	14	56 $\pm$ 19	33 $\pm$ 15	24 $\pm$ 4
	21	77 $\pm$ 2 †	69 $\pm$ 2 †‡	7 $\pm$ 3
G <sub>3</sub> RGDG <sub>6</sub> PHSRNG	4	129 $\pm$ 52	29 $\pm$ 10 §	99 $\pm$ 62 §
	7	68 $\pm$ 23	24 $\pm$ 6	44 $\pm$ 17 §
	14	57 $\pm$ 12	21 $\pm$ 9	36 $\pm$ 10
	21	74 $\pm$ 2 †	67 $\pm$ 3 †‡	7 $\pm$ 3
G <sub>3</sub> PHSRNG <sub>6</sub> RGDG	4	109 $\pm$ 16	53 $\pm$ 14 §	56 $\pm$ 5 §
	7	49 $\pm$ 11 †	21 $\pm$ 8	28 $\pm$ 3 § †
	14	87 $\pm$ 23	38 $\pm$ 12	49 $\pm$ 29
	21	60 $\pm$ 11	55 $\pm$ 8	5 $\pm$ 3 †
G <sub>3</sub> RDGG	4	91 $\pm$ 11	51 $\pm$ 1 §	40 $\pm$ 10 §
	7	66 $\pm$ 16	30 $\pm$ 11	36 $\pm$ 6 §
	14	48 $\pm$ 9 ‡	23 $\pm$ 6 ‡	25 $\pm$ 6
	21	35 $\pm$ 10 †‡§	32 $\pm$ 9 †§	4 $\pm$ 2 †
No grafted peptide	4	94 $\pm$ 32	42 $\pm$ 27 §	52 $\pm$ 16 §
	7	41 $\pm$ 10	11 $\pm$ 2 §	30 $\pm$ 6 §
	14	89 $\pm$ 21	56 $\pm$ 18	33 $\pm$ 15
	21	63 $\pm$ 4	55 $\pm$ 4	7 $\pm$ 2 †
Empty Cage	4	135 $\pm$ 22	129 $\pm$ 22	6 $\pm$ 1
	7	42 $\pm$ 8 ‡	38 $\pm$ 8 ‡	4 $\pm$ 1
	14	51 $\pm$ 10 ‡	35 $\pm$ 6 ‡	15 $\pm$ 10
	21	82 $\pm$ 22 ‡	80 $\pm$ 25 ‡	2 $\pm$ 2

All values expressed in mean  $\pm$  s.e.m., n=3. † represents  $p < 0.05$  vs respective values of “no grafted peptide” controls, § represents  $p < 0.05$  vs respective values of “empty cage” controls, and ‡ represents  $p < 0.05$  vs respective values at day 4 of the same sample type.

**Table 4.** Adherent macrophage density on cage-implanted mPEGmA-co-Ac-co-TMPTA networks grafted with various fibronectin-derived oligopeptides

Peptide	Adherent macrophage density ( $\times 10^3$ macrophages/mm <sup>2</sup> ) at various post-implantation time (days)					
	4	7	14	21	35	70
G <sub>3</sub> RGDG	138 $\pm$ 22 †	85 $\pm$ 12 †‡	33 $\pm$ 12 †‡	15 $\pm$ 3 ‡	14 $\pm$ 2 ‡	4 $\pm$ 2 ‡
G <sub>3</sub> PHSRNG	124 $\pm$ 12 †	57 $\pm$ 10 †‡	31 $\pm$ 11 †‡	10 $\pm$ 0 ‡	9 $\pm$ 1 ‡	4 $\pm$ 2 ‡
G <sub>3</sub> RGDG <sub>6</sub> PHSRNG	126 $\pm$ 8 †	58 $\pm$ 12 †‡	23 $\pm$ 4 †‡	14 $\pm$ 4 ‡	6 $\pm$ 5 ‡	0 $\pm$ 0 ‡
G <sub>3</sub> PHSRNG <sub>6</sub> RGDG	183 $\pm$ 27 †	69 $\pm$ 6 †‡	30 $\pm$ 5 †‡	16 $\pm$ 4 ‡	12 $\pm$ 5 ‡	3 $\pm$ 1 ‡
G <sub>3</sub> RDGG	75 $\pm$ 16	36 $\pm$ 5 ‡	15 $\pm$ 3 ‡	15 $\pm$ 6 ‡	9 $\pm$ 3 ‡	3 $\pm$ 2 ‡
No grafted peptide	74 $\pm$ 26	37 $\pm$ 4 ‡	14 $\pm$ 2 ‡	19 $\pm$ 3 ‡	6 $\pm$ 3 ‡	1 $\pm$ 1 ‡

All values expressed in mean  $\pm$  s.e.m., n=3. † represents  $p < 0.05$  vs respective values of “no grafted peptide” controls and ‡ represents  $p < 0.05$  vs respective values at day 4 of the same sample type.

G<sub>3</sub>PHSRNG<sub>6</sub>RGDG, or G<sub>3</sub>RDGG was comparable but was slower than that on G<sub>3</sub>RGDG and faster than that on “no grafted peptide” controls. By coupling the results of measured FBGC density and the kinetic analysis, our findings indicate that the presence of grafted G<sub>3</sub>RGDG or G<sub>3</sub>PHSRNG<sub>6</sub>RGDG on mPEGmA-co-Ac-co-TMPTA networks modulate a high level of FBGC formation by 4 days of implantation by significantly increasing both the number of macrophages that participate in the cell fusion process and the rate of cell fusion. Our *in vivo* investigations ascertained the importance of RGD and PHSRN amino acid sequences in modulating macrophage function in a time and orientation dependent fashion.

Although the *in vitro* FBGC assay system does not fully mimic the complex and dynamic host foreign body response in terms of FBGC formation, both *in vivo* and *in vitro*

results point to the important spatial relationship between RGD and PHSRN domains in mediating FBGC development as a function of time. Furthermore, the complexation between integrins and RGD and PHSRN domains of the native fibronectin molecule has been shown to be highly dependent upon the distance and the orientation between the two sequences (23,25). In our study, this distance was approximated by the linker poly-Gly hexamer in the peptide design and the orientation was controlled by the peptide grafting at the N-terminus. Although, we do not have evidences of the actual structure of our synthetic peptides in mimicking the optimal integrin binding structure of native fibronectin, our comparative analyses showed distinct differences in the activity of peptides containing these two sequences and variations thereof in modulating macrophage function.

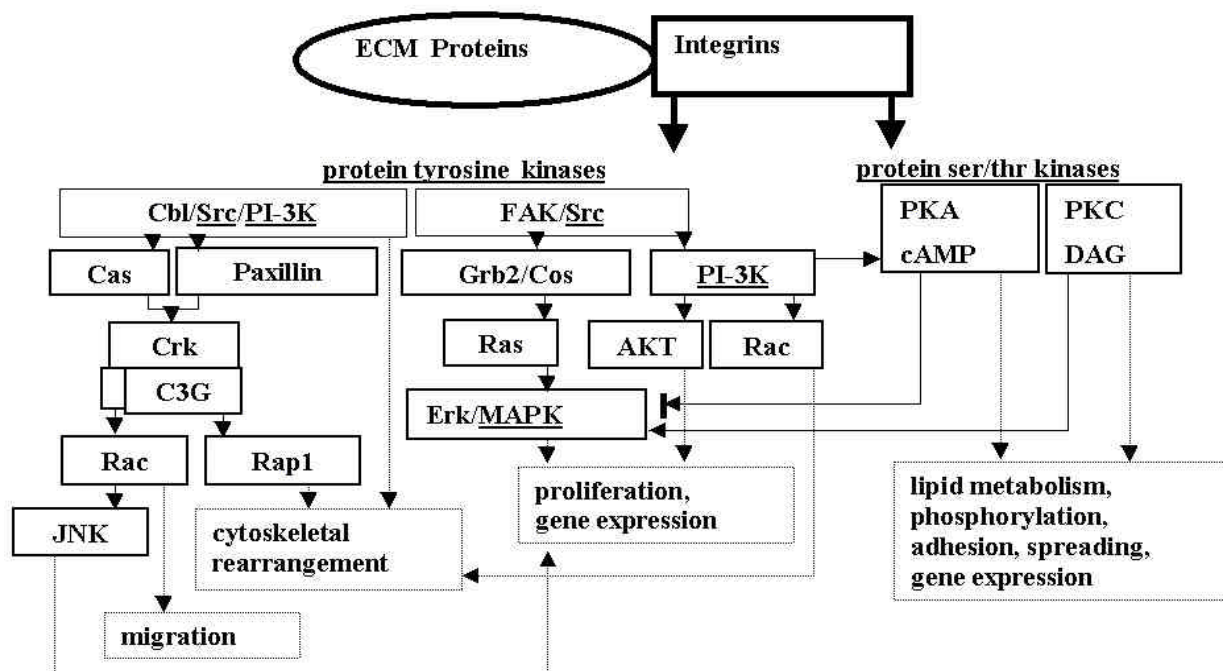


**Figure 1.** Intracellular signal transduction cascades initiated by the association of extracellular membrane integrin receptors and extracellular matrix proteins (ECM) such as fibronectin resulting in the modulation of leukocyte function and behavior.

**Table 5.** Adherent FBGC density on cage-implanted mPEGMA-co-Ac-co-TMPTA networks grafted with various fibronectin-derived oligopeptides

Peptide	Adherent FBGC density (FBGC/mm <sup>2</sup> ) at various post-implantation time (days)					
	4	7	14	21	35	70
G <sub>3</sub> RGDG	12 ± 9 †	10 ± 3 †	11 ± 4 †	11 ± 0 †	12 ± 1 †	9 ± 3 †
G <sub>3</sub> PHSRNG	0 ± 0	7 ± 1 ††	13 ± 4 ††	11 ± 1 ††	13 ± 1 ††	9 ± 2 ††
G <sub>3</sub> RGDG <sub>6</sub> PHSRNG	1 ± 1	4 ± 1 †	7 ± 1 ††	10 ± 2 ††	9 ± 1 ††	12 ± 2 ††
G <sub>3</sub> PHSRNG <sub>6</sub> RGDG	5 ± 3 †	8 ± 4 †	8 ± 1 †	7 ± 1 †	11 ± 2 †	9 ± 2 †
G <sub>3</sub> RDGG	0 ± 0	1 ± 1	3 ± 2	4 ± 1 †	5 ± 2 †	3 ± 0 †
No grafted peptide	0 ± 0	1 ± 1	2 ± 1	3 ± 1 †	3 ± 1 †	3 ± 2 †

All values expressed in mean ± s.e.m., n=3. † represents  $p < 0.05$  vs respective values of “no grafted peptide” controls and †† represents  $p < 0.05$  vs respective values at day 4 of the same sample type.

#### 4.3. Probing the intracellular signaling with biomimetic oligopeptides

Activated integrin receptors have been shown to up-regulate selected signaling molecules under a variety of ligand-receptor associations (figure 1). For example, Src is involved in integrin signaling upon ligation with extracellular matrix proteins, such as fibronectin, fibrinogen, or vitronectin, leading to macrophage adhesion and focal adhesion kinase formation. We employed fibronectin-derived adhesion-mediating peptides to further probe the differential signaling for macrophage adhesion. At an earlier culture time, the adherent density of macrophages pre-treated with H-7 was significantly lower on G<sub>3</sub>PHSRN-grafted networks than that of vehicle controls at 2 h (table 6), suggesting that the adhesion was PSK-dependent when G<sub>3</sub>PHSRN was grafted onto networks. At a later culture time (i.e. 48 h), the adherent macrophage density on G<sub>3</sub>RGDG- and G<sub>3</sub>PHSRNG-grafted networks decreased significantly with H-7 treatment when compared with respective vehicle controls. To delineate the role of specific PSK family in mediating macrophage adhesion mediated by fibronectin domains, we observed

that the inhibition of PKA and PKC did not effect macrophage adhesion at 24 h on networks grafted with fibronectin when compared with that of vehicle controls (table 7 and additional data not shown). However, G<sub>3</sub>RGDG<sub>6</sub>PHSRNG-grafted networks showed PKC-dependent macrophage adhesion but not on other surfaces (table 7). RGD and PHSRN sequences that are combined in the form of G<sub>3</sub>RGDG<sub>6</sub>PHSRNG are involved in this PKC-dependency of macrophage adhesion; furthermore, the signaling is dependent on the sequence orientation (i.e. G<sub>3</sub>RGDG<sub>6</sub>PHSRNG and not G<sub>3</sub>PHSRNG<sub>6</sub>RGDG). PKC is a family of closely related phospholipid-dependent protein kinases. Activation of IP3 kinase is thought to be an upstream event in PKC activation and is also involved in the integrin-mediated adhesion signaling. IP3-K inhibition decreased adherent macrophage density on surfaces grafted with none, G<sub>3</sub>RGDG, G<sub>3</sub>RDGG, G<sub>3</sub>RGDG<sub>6</sub>PHSRNG, or G<sub>3</sub>PHSRNG<sub>6</sub>RGDG when compared with vehicle controls (table 7). One of the downstream kinases of PKC is MEK, which is responsible for MAP kinase activation and is a double specific kinase of PTK and PSK. We found that MEK inhibition resulted in a higher macrophage adherent

**Table 6.** Effect of PTK or PSK inhibitor on adherent macrophage density on modified mPEGMA-co-Ac-co-TMPTA networks

Grafted Molecule	2hr			48hr		
	Vehicle	AG82	H-7	Vehicle	AG82	H-7
None	638 ± 246	511 ± 137	447 ± 47	207 ± 116	76 ± 48	77 ± 57
Fibronectin	462 ± 157	473 ± 150	574 ± 30	343 ± 155	117 ± 70	281 ± 242
G <sub>3</sub> RGDG	664 ± 88	613 ± 67	321 ± 154	237 ± 96	120 ± 30	66 ± 2 *
G <sub>3</sub> RDGG	568 ± 181	466 ± 245	397 ± 60	155 ± 72	72 ± 41	104 ± 11
G <sub>3</sub> PHSRNG	736 ± 50	355 ± 159	355 ± 42 *	182 ± 39	118 ± 34	70 ± 4 *
G <sub>3</sub> PHSRNG <sub>6</sub> RGDG	410 ± 60	613 ± 210	743 ± 303	113 ± 40	84 ± 46	57 ± 31

All values expressed in macrophage/mm<sup>2</sup>, mean ± s.e.m., n = 3 to 4. \* represents  $p < 0.05$  vs. respective values of “none” vehicle treatment.

**Table 7.** Effects of PKC, IP3K, or MEK inhibitor on adherent macrophage density on mPEGMA-co-Ac-co-TMPTA networks at 24hr

Grafted Molecule	Vehicle	PKC Inhibition	IP3 kinase inhibition	MEK inhibition
None	517 ± 72	705 ± 322	284 ± 87 *	662 ± 133
Fibronectin	569 ± 119	617 ± 90	532 ± 344	690 ± 27
G <sub>3</sub> RGDG	438 ± 48	618 ± 167	207 ± 59 *	487 ± 29
G <sub>3</sub> RDGG	395 ± 63	567 ± 124	226 ± 87 *	667 ± 32 *
G <sub>3</sub> PHSRNG	436 ± 48	551 ± 144	369 ± 332	725 ± 151 *
G <sub>3</sub> PHSRNG <sub>6</sub> RGDG	391 ± 65	549 ± 128	172 ± 40 *	433 ± 212
G <sub>3</sub> RGDG <sub>6</sub> PHSRNG	349 ± 80	607 ± 122 *	146 ± 76 *	638 ± 158 *

All values expressed in macrophage/mm<sup>2</sup>, mean ± s.e.m., n = 3 to 4. \* represents  $p < 0.05$  vs respective values of “none” vehicle treatment.

density on G<sub>3</sub>RDGG-, G<sub>3</sub>PHSRNG-, and G<sub>3</sub>RGDG<sub>6</sub>PHSRNG-grafted networks. Thus, MEK seems to have a negative effect on macrophage adhesion depending on the nature of ligand-receptor association. We demonstrated that the requirement of PTK and PSK activation for macrophage adhesion dynamically varied with surface ligands and culture time. The PKC-dependent adhesion was related to RGD and PHSRN sequences, and to the sequence orientation thereof in a form of G<sub>3</sub>RGDG<sub>6</sub>PHSRNG. Furthermore, we observed multiple effects of MEK in mediating adhesion, which depended on the method of ligand immobilization.

## 5. ACKNOWLEDGMENTS

The authors thank the National Institutes of Health R01 HL 63686 and the Whitaker Foundation RG99-0285.

## 6. REFERENCES

- Anderson J.M: Mechanisms of inflammation and infection with implanted devices. *Cardiovasc Pathol* 2, 33S-41S (1993)
- Anderson J.M: Inflammatory response to implants. *ASAIO* 11, 101-107 (1988)
- Ziats N.P., K.M. Miller & J.M. Anderson: *In vivo* and *in vitro* interaction of cells with biomaterials. *Biomaterials* 9, 5-13 (1988).
- Rudolph R. & D. Cheresch: Cell adhesion mechanisms and their potential impact on wound healing and tumor control. *Clin Plast Surg* 17, 457-62 (1990)
- Ziats N.P., D.A. Pankowsky, B.P. Tierney, Q.D. Ratnoff & J.M. Anderson: Adsorption of Hageman factor (factor XII) and other human plasma proteins to biomedical polymers. *J Lab Clin Med* 116, 687-696 (1990)

6. Wewers M.D. In: Cytokines in Health and Disease. Marcel Dekker, New York (1994)

7. Ward P.A: Recruitment of inflammatory cells into lung: roles of cytokines, adhesion molecules, and complement. *J Lab Clin Med* 129, 400-404 (1997)

8. Jauregui H.O: Cell adhesion to biomaterials. The role of several extracellular matrix components in the attachment of non-transformed fibroblasts and parenchymal cells. *ASAIO Trans* 33, 66-74 (1987)

9. Zhao Q., N. Topham, J.M. Anderson, A. Hiltner, G. Lodoen & C.R. Payet: Foreign-body giant cells and polyurethane biostability: *in vivo* correlation of cell adhesion and surface cracking. *J Biomed Mater Res* 25, 177-183 (1991)

10. Tang L. & J.W. Eaton: Inflammatory responses to biomaterials. *Am J Clin Pathol* 103, 66-71 (1995).

11. Meng F & C. A. Lowell: A beta 1 integrin signaling pathway involving Src-family kinases, Cbl and PI-3 kinase is required for macrophage spreading and migration. *EMBO J* 3, 4391-403 (1998)

12. Lafrenie R.M. & K.M. Yamada: Integrin-dependent signal transduction. *J Cell Biochem* 15, 543-53 (1996)

13. Graves K.L. & J. Roman: Fibronectin modulates expression of interleukin-1 beta and its receptor antagonist in human mononuclear cells. *Am J Physiol* 271(1Pt1), L61-69 (1996).

14. Simms H. & R. D'Amico: Regulation of polymorphonuclear leukocyte cytokine receptor expression: the role of altered oxygen tensions and matrix proteins. *J Immunol* 15, 3605-3616 (1996)

15. Simms H.H., R. D'Amico & K.I. Bland: Integrin stimulation regulates polymorphonuclear leukocytes inflammatory cytokine expression. *Ann Surg* 225, 757-763 (1997)
16. Zhu P., W. Xiong, G. Rodgers & E.E. Qvarnstrom: Regulation of interleukin-1 signaling through integrin binding and actin reorganization: disparate effects on NF-kappaB and stress kinase pathways. *Biochem J* 330(Pt 2), 975-981 (1998)
17. Quinn J.M., N.A. Althanasou & J.O. McGee: Extracellular matrix receptor and platelet antigens on osteoclasts and foreign body giant cells. *Histochemistry* 96, 169-176 (1991)
18. Buck C. & A.F. Horwitz: Cell surface receptors for extracellular matrix molecules. *Annu Rev Cell Biol* 3, 179-205 (1987)
19. Romberger D.J: Fibronectin. *Int J Biochem Cell Biol* 29, 939-943 (1997).
20. Potts J.R. & I.D. Campbell: Fibronectin structure and assembly. *Curr Opin Cell Biol* 6, 648-655 (1994)
21. Ruoslahti E: RGD and other recognition sequences for integrins. *Annu Rev Cell Dev Biol* 12, 697-715 (1996)
22. Aota S., M. Nomizu & K.M. Yamada: The short amino acid sequence Pro-His-Ser-Arg-Asn in human fibronectin enhances cell-adhesive function. *J Biol Chem* 269, 24756-24761 (1994)
23. Grant R.P., C. Spitzfaden, H. Altmann, I.D. Campbell & H.J. Mardon: Structural requirement for biological activity of the ninth and tenth FIII domains of human fibronectin. *J Biol Chem* 272, 6159-6166 (1997)
24. Leahy D.J., I. Aukhil & H.P. Erickson: 2.0-angstrom crystal structure of a four-domain segment of human fibronectin encompassing the RGD loop and synergy region. *Cell* 84, 155-164 (1996)
25. Spitzfaden C., R.P. Grant, H.J. Mardon & I.D. Campbell: Module-module interactions in the cell binding region of fibronectin: stability, flexibility, and specificity. *J Mol Biol* 265, 565-579 (1997)
26. Akiyama S.K: Integrins in cell adhesion and signaling. *Hum Cell* 9, 181-186 (1996)
27. Potts J.R. & I.D. Campbell: Structure and function of fibronectin modules. *Matrix Biol* 15, 313-320 (1996)
28. Kao W.J., D. Lee, J.C. Schense & J.A. Hubbell: Fibronectin modulates macrophage adhesion and FBGC formation: The role of RGD, PHSRN, and PRRARV domains. *J Biomed Mater Res* 55, 79-88 (2001)
29. Kao W.J. & D. Lee: *In vivo* modulation of host response and macrophage behavior by polymer networks grafted with fibronectin-derived biomimetic oligopeptides: the role of RGD and PHSRN domains. *Biomaterials* (in press, 2001)
30. McNally A.K., K.M. DeFife & J.M. Anderson: Interleukin-4-induced macrophage fusion is prevented by inhibitors of mannose receptor activity. *Am J Pathol* 149, 975-985 (1996)
31. Kao W.J., Q.H. Zhao, A. Hiltner & J.M. Anderson: Theoretical analysis of *in vivo* macrophage adhesion and foreign body giant cell formation on polydimethylsiloxane, low density polyethylene, and polyetherurethanes. *J Biomed Mater Res* 28, 73-79 (1994)
32. Kao W.J., A.K. McNally, A. Hiltner & J.M. Anderson: Role for interleukin-4 in foreign-body giant cell formation on a poly(etherurethane urea) *in vivo*. *J Biomed Mater Res* 29, 1267-1275 (1995)
33. WJ Kao & JM Anderson. The cage implant testing system. In: *Handbook of Biomaterials Evaluation: Scientific, Technical, and Clinical Testing of Implant Materials* (2 ed.). Ed: von Recum A, Taylor and Francis Inc., PA (1999)

**Key Words:** Host Foreign Response, Fibronectin, Biomimetics, Intracellular Signaling, Integrins, Review

**Send correspondence to:** W. J. Kao, Ph.D., School of Pharmacy and the Department of Biomedical Engineering of the College of Engineering, University of Wisconsin – Madison, Madison, WI 53705. Tel: 608-263-2998, Fax: 608-262-3397, E-mail: wjkao@pharmacy.wisc.edu